ORIGINAL PAPER

Robust adaptive beamforming with enhancing the interference suppression capability

LINXIAN LIU[1] AND YANG LI[2]

The steering vector mismatch causes signal self-nulling for adaptive beamforming when the training data contain the desired signal component. To prevent signal self-nulling, many beamformers use robust technology, which is usually equivalent to the diagonal loading approach. Unfortunately, the diagonal loading approach achieves better signal enhancement at the cost of losing its interference suppression capability, especially at high input signal-to-noise ratio. In this paper, a novel robust adaptive beamforming method is developed to improve the interference suppression capability. The proposed beamformer is based on the worst-case performance optimization technology with a new estimated steering vector and a special set parameter. Firstly, a subspace which is orthogonal to the interference's steering vector is obtained by using the interference-plus-noise covariance matrix; then a new steering vector which is orthogonal to each interference's steering vector is estimated; finally, the beamformer's weight is solved with the worst-case performance optimization technology with a special set parameter. Theoretical analysis of the interference suppression principle is analyzed in detail, and some simulation results are presented to evaluate the performance of the proposed beamformer.

I. INTRODUCTION

The minimum variance distortionless response (MVDR) beamformer is known to maximize the output signal-to-interference-plus-noise ratio (SINR) by minimizing the total beamformer output power subject to a distortionless constraint for the signal. If the training data contain the signal component, the MVDR beamformer becomes a minimum power distortionless response (MPDR) beamformer, so even a small mismatch in the signal' steering vector (SSV) and/or array covariance matrix can lead to a severe degradation of the performance [1]. In practice, such a mismatch can be caused by the pointing error [2], calibration errors [3]), unknown wavefront distortions [4], local scattering [5], moving target [6], etc. Finite sampling sequence [7] also leads to inaccurate covariance matrix. Therefore, the robustness technology [8] is required to overcome these problems. We refer to the beamformer that attempts to preserve good performance in the presence of mismatch as robust adaptive beamformer (RAB). A minimal goal for RAB is that its performance should never degrade below the performance of a conventional beamformer.

In past two decades, many technologies have been developed to improve the robustness of the MPDR beamformer against the SSV mismatch. They are mainly divided into two types. The first type technology imposes additional constraints on the beamformer to prevent or decrease the signal self-nulling, and they can be divided into two categories: (1) The SSV updating approach updates the SSV estimated from prior parameters to make it get closer to actual SSV. Many algorithms are effective, such as the eigenspace projection approach [9], the Bayesian approach [10], and the Taylor series approximation approach [11]. However, actual SSV cannot be obtained, because the parameters that the algorithm uses are not accurate. (2) The robust constrained approach does not require actual SSV. It generally uses the SSV error norm constraint or beampattern constraint, such as the worst-case performance optimization-based beamformer (WCB) [12], the covariance fitting (CF)-based beamformer [13], and the multiple uncertainty sets constraint beamformer [14]. The constrained beamformers generally have two problems: firstly, actual SSV error is difficult to obtain in practice [15]; secondly, the constraint is usually a second-order cone program problem, therefore it does not have closed-form solution [16]. Actually, most of the constrained robust adaptive beamformers turn out to be equivalent and belong to the extended class of diagonal loading (DL) approach [13]. When a RAB equivalents to

[1]School of Applied Foreign Languages, Wuhan College of Foreign Languages and Foreign Affairs, Wuhan, 430083 Wuhan, China
[2]School of Electrical and Information Engineering, Wuhan Institute of Technology, Wuhan, 430073 Wuhan, China

Corresponding author:
Linxian Liu
Email: 750900806@qq.com

the DL approach, another problem comes: the DL level is hard to choose in practice, and the RAB achieves better signal enhancement at the cost of losing its interference suppression capability, especially when the signal-to-noise ratio (SNR) is high. (2) The second type of robust technology is to eliminate or reduce the desired signal component before estimating the covariance matrix [17, 18]. Once the desired signal component is completely eliminated, the MPDR beamformer becomes an MVDR beamformer. Recently, some RABs based on the interference-plus-noise covariance matrix (INCM) reconstruction technology are proposed [2, 17, 19–21]. The performance of the INCM-based RAB is almost always close to the optimal value across a wide range of SNR and signal-to-interference ratio (SIR). Unfortunately, the performance is severely degraded when array perturbations exist.

Most of the past studies used the SINR as the measure of system performance. However, SINR is not always the best measure performance, in some applications, SIR performance is more important [22]. In this paper, we develop a novel beamformer with enhancing the interference suppression capability at high input SNR. We call the proposed RAB as interference suppression robust adaptive beamformer (ISRAB). The main idea of ISRAB is that the suppression on the interference is enhanced as the input SNR gets larger. Three technologies, INCM reconstruction, covariance fitting, and worst-case performance optimization are used in ISRAB to guarantee enhancing the interference suppression capability.

The main contributions of this paper are listed as follows: (1) A RAB with enhancing the interference suppression capability is developed; (2) The working principle of the proposed ISRAB is analyzed, the feature of the ISRAB varies adaptively with the vary of input SNR; (3) A new steering vector which is close to actual SSV as well as orthogonal to the interference is estimated, perhaps it has potential uses for other applications.

The paper is organized as follows. The signal model and background on adaptive beamforming are presented in Section II. The theatrical analysis of the proposed ISRAB and its implementation is developed in Section III. Some simulation examples are shown in Section IV. Finally, a brief conclusion is given in Section V. In the following, $E[\cdot]$, $(\cdot)^T$, $(\cdot)^H$, $(\cdot)^{-1}$, $\|\cdot\|$, and $\perp$ denote the expectation, transpose, Hermitian transpose, inverse, the two-norm, and orthogonal respectively, superscript $\hat{}$ denotes the estimated value.

II. PROBLEM FORMULATION

Considering one signal and P uncorrelated, narrowband interference impinge on a uniform linear array (ULA) with M omni-directional sensors located at x-axis in Cartesian coordinate system, $P + 1 < M$. The received data at k-th snapshot can be expressed as

$$\mathbf{x}(k) = \mathbf{a}_o s_o(k) + \sum_{i=1}^{P} \mathbf{a}_i s_i(k) + \mathbf{n}(k), \quad (1)$$

where $\mathbf{a}_o$ and $\mathbf{a}_i = \exp\{j(2\pi/\lambda)\mathbf{P}^T\mathbf{A}_i(\theta)\}$, $i = 1, \ldots, P$, are the steering vectors of the desired signal and i-th interference respectively; λ is the wavelength; $\mathbf{P} = [\mathbf{P}_1, \mathbf{P}_2, \ldots \mathbf{P}_M]$, $\mathbf{P}_m = [p_{xm}, p_{ym}, p_{zm}]^T$, $m = 1, 2, \ldots, M$, is each sensor's axis location; $\mathbf{A}_i(\theta) = [\cos(\theta_i), \sin(\theta_i), 0]^T$, θ_i is the angle between the direction-of-arrival (DOA) of i-th signal or interference and the axis of the ULA. $s_o(k)$ and $s_i(k)$ are zero-mean stationary, $\mathbf{n}(k)$ denotes the noise.

The covariance matrix of the array output is given by

$$\begin{aligned}\mathbf{R} &= E[\mathbf{x}(k)\mathbf{x}^H(k)] \\ &= \sigma_o^2 \mathbf{a}_o \mathbf{a}_o^H + \sum_{i=1}^{P} \sigma_i^2 \mathbf{a}_i \mathbf{a}_i^H + \sigma_n^2 \mathbf{I}_M,\end{aligned} \quad (2)$$

where σ_o^2, σ_i^2, and σ_n^2 denote the power of signal, i-th interference, and noise, respectively.

The problem of maximizing the output SINR is mathematically equivalent to the problem

$$\min_{\mathbf{w}} \mathbf{w}^H \mathbf{R}_{IN} \mathbf{w} \quad s.t. \quad \mathbf{w}^H \mathbf{a}_o = 1, \quad (3)$$

where $\mathbf{w} = [w_1, \ldots, w_M]^T$ is the beamformer's weight vector, $\mathbf{R}_{IN} = \sum_{i=1}^{P} \sigma_i^2 \mathbf{a}_i \mathbf{a}_i^H + \sigma_n^2 \mathbf{I}_M$ is the actual INCM. The solution of (3) is the MVDR beamformer

$$\mathbf{w}_{opt} = \alpha \mathbf{R}_{IN}^{-1} \mathbf{a}_o, \quad (4)$$

where $\alpha = (\mathbf{a}_o^H \mathbf{R}_{IN}^{-1} \mathbf{a}_o)^{-1}$ is a normalization constant which does not affect the output SINR.

When the receiving snapshots include the desired signal component, $\mathbf{R}_{IN}$ in (4) is replaced by $\mathbf{R}$, then the MVDR becomes the MPDR: $\mathbf{w}_{MPDR} = \alpha \mathbf{R}^{-1} \mathbf{a}_o$, where $\alpha = (\mathbf{a}_o^H \mathbf{R}^{-1} \mathbf{a}_o)^{-1}$. Although the MPDR has the same SINR performance with the MVDR, however, we cannot obtain two accurate parameters in practice. On one hand, since $\mathbf{R}$ is unknown in practice, it is replaced by K-snapshots sample covariance matrix $\hat{\mathbf{R}} = (1/K)\sum_{k=1}^{K} \mathbf{x}(k)\mathbf{x}^H(k)$. On the other hand, many factors can lead to the steering vector mismatch, such as the pointing error and the array perturbations (the perturbations often include the array element position error, calibration magnitude error, and calibration phase error), they can be modeled as [23]

$$\begin{aligned}\mathbf{a}_i(\theta) &= (1 + \Delta g)e^{j\Delta\phi}e^{j(2\pi/\lambda)(\mathbf{P}+\Delta\mathbf{P})^T\mathbf{A}_i(\theta+\Delta\theta)} \\ \Delta\mathbf{P} &= [\Delta\mathbf{P}_1, \Delta\mathbf{P}_2, \ldots \Delta\mathbf{P}_M] \\ \Delta\mathbf{P}_m &= [\Delta_{xm}, \Delta_{ym}, \Delta_{zm}]^T, m = 1, 2, \ldots, M\end{aligned} \quad (5)$$

where $\Delta\theta$, Δg, $\Delta\phi$, and $\Delta\mathbf{P}$ denote the pointing error, calibration magnitude error, calibration phase error, and array element position error, respectively. In this paper, we focus on the steering vector error, so the influence of covariance matrix is omitted, thus we do not distinguish $\mathbf{R}$ and $\hat{\mathbf{R}}$ in the following.

The inaccurate of covariance matrix of steering vector can lead to the output SINR significant decrease which is called self-nulling, especially when the input SNR is high. Many robust technologies have been developed to deal with this problem, one of the most popular method is called DL.

The DL technique augments the diagonal of the covariance with a constant level

$$\mathbf{w}_{DL} = (\mathbf{R}_{IN} + \beta \mathbf{I})^{-1} \mathbf{a}_o, \tag{6}$$

where β is the DL level.

The DL technology has many useful effects, such as making the covariance matrix invertible, constraining the white noise gain [24], robust against the steering vector error and the covariance matrix error [25], etc. However, the DL technology has some problems such as the DL level is hard to be chosen [24] and the interference suppression capability is reduced [22]. Some robust adaptive beamformers, such as the famous WCB and CFRCB have been proved and belong to the class of DL technology [12, 13], therefore they have the same problems.

Most of the past studies used the SINR as the measure of system performance. However, SINR is not always the best measure performance, in some applications, SIR performance is more important [22]. In the following, we develop a novel beamformer ISRAB with enhancing the interference suppression capability.

III. THE PROPOSED BEAMFORMER

The ISRAB is developed with three steps: the INCM reconstruction technology is used to construct a subspace which is orthogonal to the interference; the CF technology is used to estimate an SV which is close to the desired signal's SV as well as orthogonal to the interference; the WCB technology is used to solve the weight vector to prevent self-nulling. Although three exist technologies are used, the form or usage in ISRAB is difference from their original complete solution.

A) Interference orthogonal subspace construction

Firstly, the INCM $\mathbf{R}_{IN}$ is reconstructed with $\mathbf{R}$ through [17]

$$\mathbf{R}_{IN} = \frac{1}{N} \sum_{i=1}^{N} \frac{\hat{\mathbf{a}}(\theta_i)\hat{\mathbf{a}}^H(\theta_i)}{\hat{\mathbf{a}}^H(\theta_i)\hat{\mathbf{R}}^{-1}\hat{\mathbf{a}}(\theta_i)}, \theta_i \in \bar{\Theta}, \tag{7}$$

where $\hat{\mathbf{a}}(\theta_i)$ is the presumed steering vector corresponding to direction θ_i, $\bar{\Theta}$ denotes the complement of signal uncertainty region Θ.

Taking the eigen-decomposition of $\mathbf{R}_{IN}$

$$\begin{aligned} \mathbf{R}_{IN} &= \mathbf{E}_I \Gamma_I \mathbf{E}_I^H + \mathbf{E}_N \Gamma_N \mathbf{E}_N^H \\ &= \sum_{i=1}^{P} \gamma_i \mathbf{e}_i \mathbf{e}_i^H + \gamma_n \sum_{i=P+1}^{M} \mathbf{e}_i \mathbf{e}_i^H, \end{aligned} \tag{8}$$

where γ_i and $\mathbf{e}_i$ are the eigenvalues and corresponding eigenvectors of $\mathbf{R}_{IN}$, the eigenvalues are sorted in descending order $\gamma_1 \geq \ldots \geq \gamma_P \gg \gamma_{P+1} = \ldots = \gamma_M = \sigma_n^2$, $\mathbf{E}_I = [\mathbf{e}_1, \ldots, \mathbf{e}_P]$ spans the interference subspace,

$\mathbf{E}_N = [\mathbf{e}_{P+1}, \ldots, \mathbf{e}_M]$ spans the noise subspace. The following formulas hold

$$\text{span}\{\mathbf{a}_i\} = \text{span}\{\mathbf{e}_i\}, i = 1, \ldots, P, \tag{9}$$

$$\mathbf{E}_I \perp \mathbf{E}_N, \mathbf{E}_I \mathbf{E}_I^H + \mathbf{E}_N \mathbf{E}_N^H = \mathbf{I}. \tag{10}$$

Therefore, the subspace $\mathbf{E}_N = [\mathbf{e}_{P+1}, \ldots, \mathbf{e}_M]$ is orthogonal to each ISV.

B) Steering vector estimation

When the angular separation between signal and interference is larger than a beam width, $\left|\mathbf{a}_o^H \mathbf{a}_i / M\right|^2 \ll 1$, $i = 1, \ldots, P$ [26]. Assuming this condition always holds, we can make the approximation $\left|\mathbf{a}_o^H \mathbf{e}_i\right|^2 \ll M$, $i = 1, \ldots, P$, and $\mathbf{a}_o^H \mathbf{E}_I \mathbf{E}_I^H \mathbf{a}_o \ll M$, which can be further extended to $\mathbf{a}_o^H \mathbf{E}_N \mathbf{E}_N^H \mathbf{a}_o = \mathbf{a}_o^H (\mathbf{I} - \mathbf{E}_I \mathbf{E}_I^H) \mathbf{a}_o = M - \mathbf{a}_o^H \mathbf{E}_I \mathbf{E}_I^H \mathbf{a}_o \approx M$. Therefore, we can make $\left\|\mathbf{E}_N^H \mathbf{a}_o\right\|^2 \approx M$. Because $\|\mathbf{a}_o\|^2 = M$, $\mathbf{a}_o$ approximately belongs to the subspace $span\{\mathbf{e}_i\}$, $i = P + 1, \ldots, M$. Hence, we can express the new SSV with the linear combination of $\mathbf{e}_i$, $i = P + 1, \ldots, M$

$$\hat{\mathbf{a}}_o \approx \mathbf{E}_N \mathbf{b}, \tag{11}$$

where $\mathbf{b}$ is an $(M - P) \times 1$ dimensional rotating vector.

The CF technology [13] can be used to solve $\mathbf{b}$

$$\min_{\hat{\mathbf{a}}_o} \hat{\mathbf{a}}_o^H \mathbf{R}^{-1} \hat{\mathbf{a}}_o \quad s.t. \quad \left\|\hat{\mathbf{a}}_o\right\|^2 = M. \tag{12}$$

Using (11) and $\mathbf{E}_N^H \mathbf{E}_N = \mathbf{I}_{M-P}$, equation (12) becomes

$$\min_{\mathbf{b}} \mathbf{b}^H \mathbf{R}_E \mathbf{b} \quad s.t. \quad \mathbf{b}^H \mathbf{b} = M, \tag{13}$$

where $\mathbf{R}_E = \mathbf{E}_N^H R^{-1} \mathbf{E}_N$. The vector $\mathbf{b}$ can be solved by the Lagrange multiplier method

$$f(\mathbf{b}, \eta) = \mathbf{b}^H \mathbf{R}_E \mathbf{b} + \eta(\mathbf{b}^H \mathbf{b} - M), \tag{14}$$

where η is the Lagrange multiplier. Differentiating of (14) with respect to $\mathbf{b}$ and equating the result to zero, the solution to (13) is given by the following generalized eigenvalue problem

$$\mathbf{R}_E \mathbf{b} = \eta \mathbf{b}. \tag{15}$$

The solution to (15) is

$$\mathbf{b} = \mathcal{M}\{\mathbf{R}_E\}, \tag{16}$$

where $\mathcal{M}\{\boldsymbol{\cdot}\}$ is the operator that yields the eigenvector corresponding to the minimal eigenvalue.

Notice that the vector should be scaled to guarantee $\left\|\hat{\mathbf{a}}_o\right\| = \sqrt{M}$. Therefore, the estimated new SSV is given by

$$\hat{\mathbf{a}}_o = \sqrt{M} \mathbf{E}_N \mathbf{b} / \|\mathbf{E}_N \mathbf{b}\|. \tag{17}$$

Obviously, $\hat{\mathbf{a}}_o$ is close to actual SSV as well as orthogonal to each ISV.

We make the following two remarks:

Remark 1. *Estimating an accurate noise subspace in* (8) *is not necessary. We can choose the eigenvectors corresponding*

to $P_{EN}(P_{EN} \leq M - P)$ small eigenvalues as the columns of $\mathbf{E}_N$. The weak interference component corresponding to the eigenvalues between P_{EN} and $M - P$ can be suppressed. An easy way to estimate P_{EN} is to choose a maximal value of P_{EN} which satisfies that the value of $\sum_{i=1}^{M-P_{EN}} \gamma_i$ divided by $\sum_{i=1}^{M} \gamma_i$ is larger than a fixed value, such as 0.9.

Remark 2. *The CF approach in* [13] *subjects to the constraint* $\left\| \mathbf{a}_{CF} - \hat{\mathbf{a}}(\hat{\theta}_o) \right\|^2 \leq \varepsilon$ *to search the maximal spatial power in SSV uncertainty region, where* $\hat{\theta}_o$ *is the presumed DOA of signal. The objective function of* (12) *searches the max spatial power through all the directions. Since* $\mathbf{E}_N \mathbf{b}$ *is orthogonal to the ISV,* $\hat{\mathbf{a}}_o$ *will not converge to any ISV. If SNR is high,* $\hat{\mathbf{a}}_o$ *will converge to the SSV. If SNR is very low, the signal power is submerged by the noise power in spatial spectrum,* $\hat{\mathbf{a}}_o$ *may converge to a noise power peak. The following stopping criterion is used to avoid that* $\hat{\mathbf{a}}_o$ *converges to the noise peak which is far from actual signal DOA: if* $\left| \hat{\mathbf{a}}_o^H \hat{\mathbf{a}}(\hat{\theta}_o) \right| < \min\{ \left| \hat{\mathbf{a}}_o^H \hat{\mathbf{a}}(\hat{\theta}_o + \theta_W/2) \right|, \left| \hat{\mathbf{a}}_o^H \hat{\mathbf{a}}(\hat{\theta}_o - \theta_W/2) \right| \}$, *setting* $\hat{\mathbf{a}}_o = \hat{\mathbf{a}}(\hat{\theta}_o)$, *where* θ_W *is the signal's DOA uncertainty range* [27] . *The criterion means that if the corresponding angle of* $\hat{\mathbf{a}}_o$ *is beyond the signal DOA uncertainty range, using initial value* $\hat{\mathbf{a}}(\hat{\theta}_o)$ *as* $\hat{\mathbf{a}}_o$.

C) Solving the weight

The worst-case performance optimization-based beamformer can be formulated as [12]

$$\begin{cases} \min_{\mathbf{w}} \mathbf{w}^H \mathbf{R} \mathbf{w} \\ s.t. \ \left| \mathbf{w}^H (\hat{\mathbf{a}}_o + \delta) \right| \geq 1, \forall \|\delta\| \leq \varepsilon \end{cases}, \quad (18)$$

where δ is the vector of the unknown mismatch between the actual SSV and its presumed value $\hat{\mathbf{a}}_o$ with a prior known norm bound ε. The solutions to (18) belongs to the DL approach [28]

$$\mathbf{w} = (\mathbf{R} + \varepsilon/\tau \ \mathbf{I}_M)^{-1} \hat{\mathbf{a}}_o, \quad (19)$$

where τ is the root to

$$\sum_{i=0}^{M-1} \frac{\left| \mathbf{q}_i^H \hat{\mathbf{a}}_o \right|^2}{(\varepsilon + \tau \lambda_i)^2} = 1, \quad (20)$$

where $\mathbf{R} = \sum_{i=0}^{M-1} \lambda_i \mathbf{q}_i \mathbf{q}_i^H$, λ_i and $\mathbf{q}_i$ are the eigenvalues and corresponding eigenvectors of $\mathbf{R}$, λ_i are sorted in descending order $\lambda_o \geq \lambda_1 \geq \ldots \geq \lambda_{P+1} = \ldots = \lambda_{M-1} = \lambda_n$. The binary search technique [28] can be used to solve (20).

D) Working principle

Eigenvectors in noise subspace are approximately orthogonal to $\hat{\mathbf{a}}_o$

$$\mathbf{q}_i^H \hat{\mathbf{a}}_o \approx 0, \ i = P + 1, \ldots, M - 1. \quad (21)$$

In the following, we assume that the interference's number is equal to one so as to obtain a theoretical result.

Simulation example 1 will show that when the interference number is larger than one, the theoretical result also establishes. The $\mathbf{R}$ with only one interference can be expressed in eigen-decomposition form

$$\mathbf{R} = \lambda_o \mathbf{q}_o \mathbf{q}_o^H + \lambda_1 \mathbf{q}_1 \mathbf{q}_1^H + \sum_{i=2}^{M-1} \lambda_n \mathbf{q}_i \mathbf{q}_i^H$$

$$= (\lambda_o - \lambda_n) \mathbf{q}_o \mathbf{q}_o^H + (\lambda_1 - \lambda_n) \mathbf{q}_1 \mathbf{q}_1^H + \lambda_n \mathbf{I}_M. \quad (22)$$

Meanwhile, $\mathbf{R}$ can be expressed in array signal form

$$\mathbf{R} \approx \sigma_o^2 \hat{\mathbf{a}}_o \hat{\mathbf{a}}_o^H + \sigma_1^2 \mathbf{a}_1 \mathbf{a}_1^H + \sigma_n^2 \mathbf{I}_M. \quad (23)$$

By combining (22) and (23), λ_o and λ_1 can be solved [26]

$$\lambda_o = \sigma_n^2 + \frac{M}{2} \left[\sigma_o^2 + \sigma_1^2 \right. $$
$$\left. + \sqrt{(\sigma_o^2 + \sigma_1^2)^2 - 4\sigma_o^2 \sigma_1^2 (1 - |v|^2)} \right], \quad (24)$$

$$\lambda_1 = \sigma_n^2 + \frac{M}{2} \left[\sigma_o^2 + \sigma_1^2 \right. $$
$$\left. - \sqrt{(\sigma_o^2 + \sigma_1^2)^2 - 4\sigma_o^2 \sigma_1^2 (1 - |v|^2)} \right], \quad (25)$$

$$\left| \mathbf{q}_i^H \hat{\mathbf{a}}_o \right|^2 = M(-1)^{i+1} \frac{-\lambda_i + M\sigma_1^2 (1 - |v|^2)}{\lambda_o - \lambda_1}, i = 0, 1, \quad (26)$$

where $\lambda_o > \lambda_1$, $|v|^2 = \left| \hat{\mathbf{a}}_o^H \mathbf{a}_i / M \right|^2 \ll 1$, which is similar with the condition presented in Section III.B.

Case 1: Very high SNR

If $\sigma_o^2 \gg \sigma_1^2$, we can make

$$\left| \mathbf{q}_o^H \hat{\mathbf{a}}_o \right|^2 \approx M, \left| \mathbf{q}_1^H \hat{\mathbf{a}}_o \right|^2 \approx 0. \quad (27)$$

If ε approaches $\sqrt{M}$ (we set $\varepsilon = 0.99\sqrt{M}$ in the following), the denominators of (20) can satisfy

$$(\varepsilon + \tau \lambda_i)^2 > M, \quad i = 0, 1, \ldots, P. \quad (28)$$

From (20), (21), (27), and (28) we have

$$1 = \sum_{i=0}^{M-1} \frac{\left| \mathbf{q}_i^H \hat{\mathbf{a}}_o \right|^2}{(\varepsilon + \tau \lambda_i)^2} \approx \frac{\left| \mathbf{q}_o^H \hat{\mathbf{a}}_o \right|^2}{(\varepsilon + \tau \lambda_o)^2} \approx \frac{M}{(\varepsilon + \tau \lambda_o)^2}. \quad (29)$$

Equation (29) further reveals that

$$\frac{\varepsilon}{\tau \lambda_o} \approx \frac{\varepsilon}{\sqrt{M} - \varepsilon} = 99, \quad for \ \varepsilon = 0.99\sqrt{M}. \quad (30)$$

Equation (30) indicates that the equivalent DL level in (19) $\varepsilon/\tau = 99\lambda_o$ is much greater than the largest eigenvalue λ_o. Hence the effect of the weight vector (19) on the ISV is

$$\mathbf{w}^H \mathbf{a}_1 = \hat{\mathbf{a}}_o^H \sum_{i=0}^{M-1} \left(\lambda_i + \frac{\varepsilon}{\tau} \right)^{-1} \mathbf{q}_i \mathbf{q}_i^H \mathbf{a}_1$$

$$\approx \hat{\mathbf{a}}_o^H \frac{\tau}{\varepsilon} \sum_{i=0}^{M-1} \mathbf{q}_i \mathbf{q}_i^H \mathbf{a}_1 = \frac{1}{99\lambda_o} \hat{\mathbf{a}}_o^H \mathbf{a}_1. \quad (31)$$

In case of the SNR is very large, the attenuation by $1/(99\lambda_o)$ and the orthogonality between $\hat{\mathbf{a}}_o$ and $\mathbf{a}_1$ doubly make the value of $\left| \mathbf{w}^H \mathbf{a}_1 \right|$ very small, which means the interference can be significantly suppressed.

Case 2: Very low SNR

If $\sigma_o^2 \ll \sigma_1^2$, we can make $|\mathbf{q}_o^H \hat{\mathbf{a}}_o|^2 \approx 0$, $|\mathbf{q}_1^H \hat{\mathbf{a}}_o|^2 \approx M$, and then $\varepsilon/\tau = 99\lambda_1$, through the same way with (22) to (30). In very low SNR case, $\lambda_1 \approx \sigma_n^2$, therefore the DL level in (19) is about $\varepsilon/\tau = 99\sigma_n^2$. Therefore, the ISRAB equivalents to the DL beamformer with level $99\sigma_n^2$.

It can be concluded that, the feature of the ISRAB varies adaptively with the vary of input SNR.

E) Implementation

The implementation of ISRAB is summarized as follows

Step 1: Reconstructing the INCM $\mathbf{R}_{IN}$ by (7).
Step 2: Taking the eigen-decomposition of $\mathbf{R}_{IN}$ by (12) to obtain the subspace $\mathbf{E}_N$.
Step 3: Calculating $\hat{\mathbf{a}}_o$ by (8): $\hat{\mathbf{a}}_o = \mathbf{E}_N \mathcal{M}\{\mathbf{E}_N^H \mathbf{R}^{-1} \mathbf{E}_N\}$, $\hat{\mathbf{a}}_o = \sqrt{M}\hat{\mathbf{a}}_o / \|\hat{\mathbf{a}}_o\|$.
Step 4: Calculating $\mathbf{w} = (\mathbf{R} + \varepsilon/\tau \mathbf{I}_M)^{-1}\hat{\mathbf{a}}_o$, where τ is the root to (20).

The implementation mainly includes the reconstructing of the INCM, the eigen-decomposition, and the matrix inversion, their computational time complexity are $O(NM^2)$, $O(M^3)$, and $O(M^3)$, respectively.

IV. SIMULATION EXAMPLES

The array is a ULA with half-wavelength spacing d and $M=16$ elements. There are two interference with directions and interference-to-noise ratios (INRs) of [$40°$, 20 dB] and [$110°$, 30 dB], respectively. The signal and interference are assumed as point sources except for Example 3. The additive noise is a spatially white Gaussian process. The desired signal's actual DOA is $80°$, whereas its estimated value $\hat{\theta}_o$ is $82°$. The signal DOA uncertainty range is $\theta_W = 8°$, which means the signal uncertainty region Θ is [$78°$, $86°$]. The degree step is set to $1°$ in INCM reconstruction, which indicates $N = 180$ for implementation Step 1. Assuming Δg, $\Delta \phi$, and $\Delta_{xm}, \Delta_{ym}, \Delta_{zm}$, $m = 1, 2, \ldots, M$, are statistically independent, zero-mean, Gaussian random variables. Δg, $\Delta \phi/\pi$, and Δ_{xm}/d, Δ_{ym}/d, Δ_{zm}/d have the same standard deviation σ_Δ. We set $\sigma_\Delta = 0$ for perfectly calibrated array in Section IV.A, and set $\sigma_\Delta = 0.02$ for array perturbation in Section IV.B. The number of snapshots is 100 except for Example 7. 100 independent runs are performed except for Example 5 and Example 10.

The performance of the ISRAB is compared with the following classic beamformers:

(1) OPT: the MVDR beamformer of (4) with actual covariance matrix and actual SSV.
(2) ISRAB: the proposed beamformer with $\varepsilon = 0.99\sqrt{M}$.
(3) FDL: the DL beamformer $\mathbf{w}_{DL} = (\mathbf{R} + \beta\mathbf{I})^{-1}\hat{\mathbf{a}}(\hat{\theta}_o)$, with a fixed DL level $\beta = 99\sigma_n^2$.
(4) VDL: the beamformer of [29].
(5) WCB: the beamformer of [12] with $\varepsilon = 0.5\sqrt{M}$.
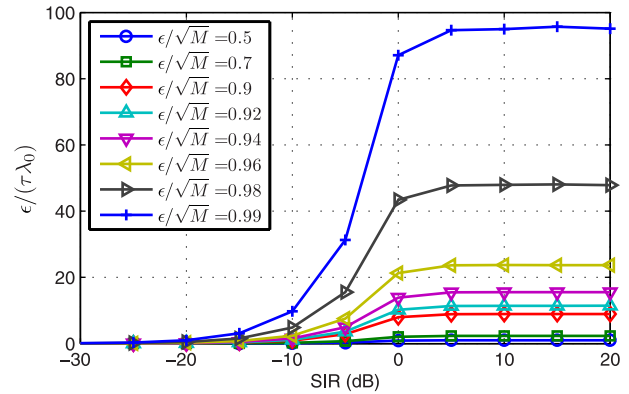(6) IWCB: the beamformer of [16] with $\varepsilon = 0.2$.

Fig. 1. The DL level divided by maximal eigenvalue versus SIR.

(7) RIN: the beamformer of [17], $\mathbf{w}_{RIN} = \mathbf{R}_{IN}^{-1}\mathbf{a}_o$, where $\mathbf{R}_{IN}$ is calculated by (7), and we use actual SSV directly instead of estimating it with the CVX tool.
(8) CFRIN: the beamformer of [19] with $\varepsilon = 0.2$.

The main computational time complexity of implementation is $O(NM^2)$ for ISRAB, RIN, CFRIN, and is $O(M^3)$ for others. Generally $M \ll N$. The dominant computational complexity of the ISRAB is $O(NM^2)$ which is determined by the INCM reconstruction step, it can be reduced to $O(M^3)$ if the INCM reconstruction method in [21] is used.

A) Perfect calibrated array

Example 1. *DL level. In Section III.C, we assume that the interference number is equal to one so as to obtain a theory result. Figure 1 displays the DL level divided by maximal eigenvalue versus SIR when the interference number is greater than one. Results shows that when the input SNR is greater than the INR, the DL level ε/τ corresponding to $\varepsilon \geq 0.99\sqrt{M}$ is much greater than the maximal eigenvalue λ_o of R.*

Example 2. *Noise subspace. Figure 2 displays the error between the estimated SSV $\hat{\mathbf{a}}_o$ and actual SSV $\mathbf{a}_o$ versus SNR and dimension of $\mathbf{E}_N$. As discussed in Remark 2, $\hat{\mathbf{a}}_o$ is set equal to $\hat{\mathbf{a}}(\hat{\theta}_o)$ at very low SNR, hence the error is reduced to about $\min_\varphi \left\| \hat{\mathbf{a}}(\hat{\theta}_o)e^{j\varphi} - \mathbf{a}_o \right\| = 1.95$ at very low SNR. When the SNR is > -12 dB, which approximately equals to the noise power, $\hat{\mathbf{a}}_o$ is closer to $\mathbf{a}_o$ than $\hat{\mathbf{a}}(\hat{\theta}_o)$. The actual dimension of noise subspace $\mathbf{E}_N$ is 14, when estimated dimension P_{EN} is between 9 and 14, $\hat{\mathbf{a}}_o$ is stable, which verifies the Remark 1 is reasonable.*

Example 3. *SINR versus SNR. Figure 3 displays the output SINR versus SNR with $2°$ pointing error. Results show that: (1) The output SINR of VDL degrades quickly when SNR is >0 dB while the SINR of FDL degrades when SNR is >10 dB, hence, the DL level with $99\sigma_n^2$ is better than variable DL level in this case; (2) The SINR of WCB and IWCB bias from OPT when SNR is large, it is because the suppress capability of interference is decrease as the SNR gets larger. (3) The SINRs of RIN and CFRIN are close to OPT value, but a litter lower*
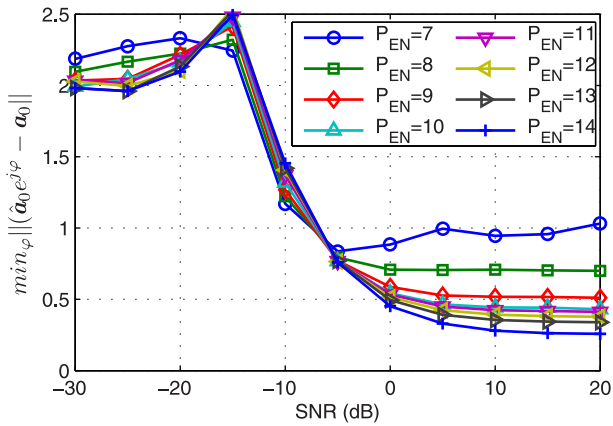
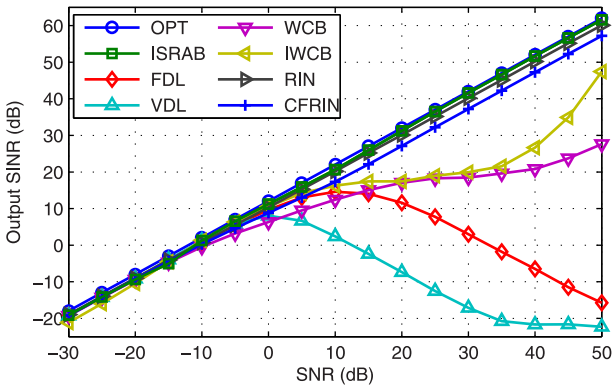**Fig. 2.** The error of estimated SSV versus SNR.

Fig. 4. Output SIR versus SNR.

Fig. 3. Output SINR versus SNR.

Fig. 5. Array pattern.

than the proposed ISRAB, the reason is analyzed in our previous work [30]: the main peak of RIN and CFRIN cannot point to actual signal's direction even if the steering vector is accurate (also see Example 5).

Example 4. *SIR versus SNR. Figure 4 displays the output SIR versus SNR with 2° pointing error. Results show that: (1) The suppress capability of interference is decrease for the FDL, VDL, WCB, and IWCB when SNR is larger than 0 dB. (2) The SIR of RIN is stable through all the SNR, but a little lower than ISRAB and CFRIN especially when the SNR is very low and very high. (3) The SIR of ISRAB is higher than others expect a slight lower than the CFRCB when SNR is high.*

Example 5. *Array pattern. Figure 5 shows the array pattern of four beamformers at SNR=25 dB. Results show that: (1) Both the ISRAB and RIN form deeper nulls at interference directions than WCB. (2) The ISRAB can point the main beam peak to actual signal direction, while both the RIN and WCB deviate to the actual signal direction, even if the RIN uses actual SSV. (3) There exists self-nulling for FDL. The defect of RIN is explained as follows [30]: the $\mathbf{R}_{IN}$ in (7) contains no signal or noise component in Θ, hence the optimization condition $\min \mathbf{w}^H \mathbf{R}_{IN} \mathbf{w}$ in (3) has no effect in Θ. The constraint $\mathbf{w}^H \mathbf{a}(\theta) = 1$ guarantees that the beampattern gain is equal to one at direction θ, but the gain at other discrete*
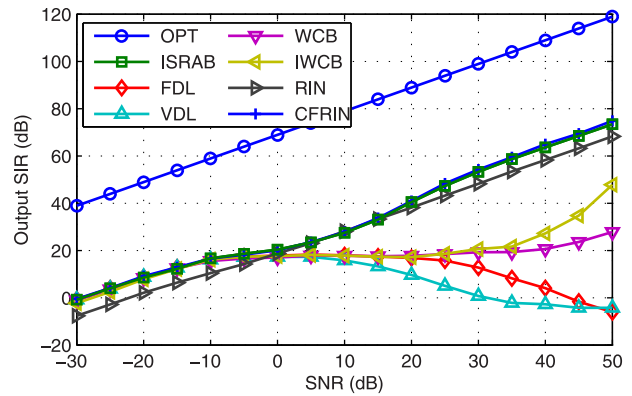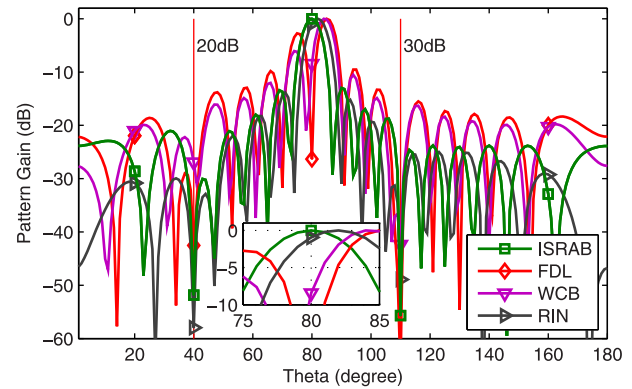
directions in Θ may exceed one without enlarging $\mathbf{w}^H \mathbf{R}_{IN} \mathbf{w}$. Then the main lobe peak of beampattern may point to another direction, thus the SINR of RIN degrades slightly. The ISRAB does not have the optimization condition $\min \mathbf{w}^H \mathbf{R}_{IN} \mathbf{w}$, its weight vector equivalents to $\hat{\mathbf{a}}_o$ which is very close to actual SSV (as shown in Fig. 2), so the main beam of ISRAB can point (very close) to actual signal's directions. Because the solution of WCB is equivalent to the DL, the peak of the main beam is moved with the DL level when there exists a pointing error [31].

Example 6. *Pointing error. Figure 6 displays the output SINR versus pointing error, SNR=25 dB. Results show that: (1) Whether FDL or VFL is not suitable in this scenario. (2) We set $\varepsilon = 2$ for WCB, which corresponds to about 2° pointing error. the SINR of WCB performs stable when pointing error is less than 2°, but degrades greatly when the pointing error is larger than 2°. (3) When the pointing error is $< \theta_W/2 = 4°$, ISRAB performs stably, and its SINR is the closest to OPT. (4) It is because the stopping criterion in Remark 2 causes the SINR of ISRAB decrease when the pointing error is larger than 4°, the CFRIN has the same stopping criterion while the RIN does not have.*

Example 7. *Snapshots. Figure 7 displays the output SINR versus snapshots at SNR = 25 dB. Results shows that the performance of ISRAB tends to be stable when the number of*
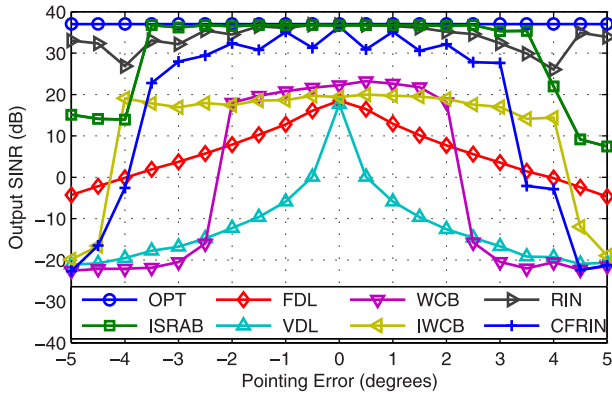
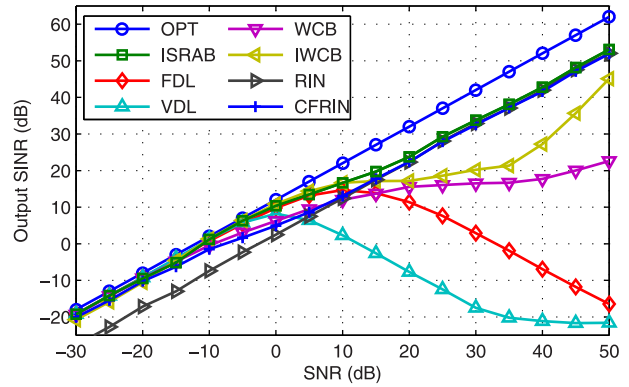**Fig. 6.** Output SINR versus pointing error.
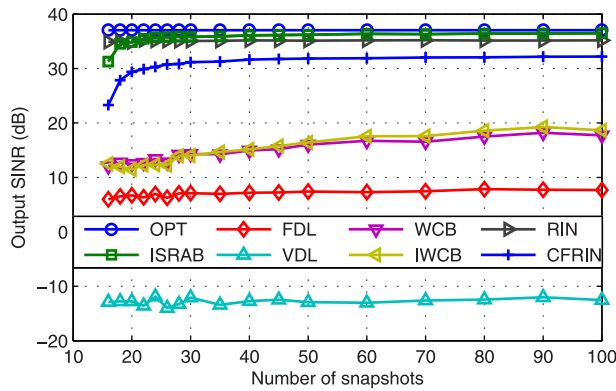

Fig. 8. Output SINR versus SNR.

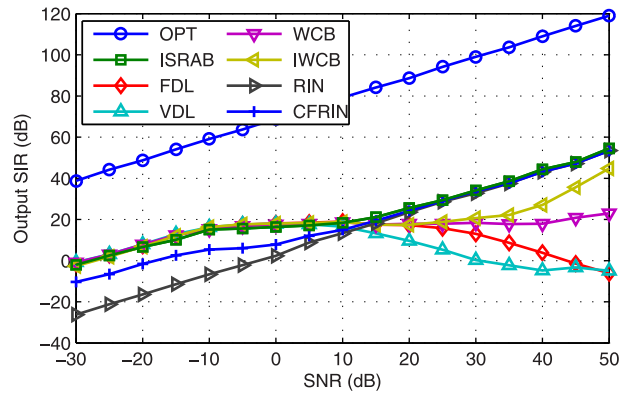**Fig. 7.** Output SINR versus snapshots.

Fig. 9. Output SIR versus SNR.

snapshots is larger than 20. The SINR performance is not good with small snapshots is a drawback of the ISRAB, as well as the CFRIN.

B) Array perturbations

In the following examples, the SV mismatch is caused by both $2°$ pointing error, and array perturbations with $\sigma_\Delta = 0.02$.

Example 8. *SINR versus SNR. Figure 8 shows the output SINR versus SNR. Compared with Fig. 3, the SINR of RIN degrades with a fixed value through all the SNRs in Fig. 8. The SINR of ISRAB is very close to OPT at low SNR, although it degrades at high SNR, it is always better than other beamformers.*

Example 9. *SIR versus SNR. Figure 9 displays the output SIR versus SNR with pointing error and array perturbations. Compared with Fig. 4, the SIRs of RIN and CFRIN are decreased at low SNR case, the SIR of ISRAB almost outperforms others through all the SNRs.*

Example 10. *Array pattern. Figure 10 displays the array pattern at SNR = 25 dB. The ISRAB can point the main lobe peak closest to actual signal direction than RIN and WCB. Although the nulling depths at interference directions*
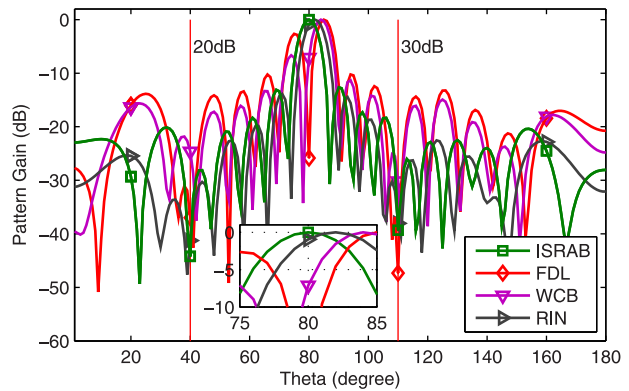

Fig. 10. Array pattern.

of ISRAB are lower than that of Fig. 3, they are much deeper than WCB in this scenario.

Finally, the main advantages of the proposed ISRAB are summarized as follows: (1) The nulling at interference is much deeper; (2) The main peak can point to signal's actual directions; (3) All the parameters are fixed in any situations.

V. CONCLUSION

A novel robust adaptive beamformer ISRAB has been developed. Three steps processing are performed to guarantee that the beamformer's weight is orthogonal to each ISV and

does not suppress the desired signal as an interference. Theoretical analysis of the interference suppression principle is analyzed in detail. Some special set of parameters are also analyzed. Simulation results show that, compared with several classical beamformers, the proposed ISRAB has the advantages in many cases, such as the pointing error and array perturbations.

STATEMENT OF INTEREST

The authors declare no conflict of interest.

REFERENCES

[1] Wax, M.; Anu, Y.: Performance analysis of the minimum variance beamformer in the presence of steering vector errors. *IEEE Trans. Signal. Process.*, **44** (4) (1996), 938–947.

[2] Liu, F.; Jian, W.; Du, R.; Bai, X.: Robust adaptive beamforming against the array pointing error, in *Progress in Electromagnetics Research Symposium-fall*, 2018, 2782–2789.

[3] Tseng, C.-Y.; Feldman, D.D.; Griffiths, L.J.: Steering vector estimation in uncalibrated arrays. *IEEE Trans. Signal. Process.*, **43** (6) (1995), 1397–1412.

[4] Weiss, A.J.; Friedlander, B.: Fading effects on antenna arrays in cellular communications. *IEEE Trans. Signal. Process.*, **45** (5) (1997), 1109–1117.

[5] Pedersen, K.I.; Mogensen, P.E.; Fleury, B.H.: A stochastic model of the temporal and azimuthal dispersion seen at the base station in outdoor propagation environments. *IEEE Trans. Veh. Technol.*, **49** (2) (2000), 437–447.

[6] Yermeche, Z.; Grbic, N.; Claesson, I.: Beamforming for moving source speech enhancement, in *Applications of Signal Processing to Audio and Acoustics, 2005. Workshop on* IEEE, October 2005, 25–28.

[7] Mestre, X.; Lagunas, M.A.: Finite sample size effect on minimum variance beamformers: optimum diagonal loading factor for large arrays. *IEEE Trans. Signal. Process.*, **54** (1) (2006), 69–82.

[8] Li, J.; Stoica, P.: Robust Adaptive Beamforming. Wiley Online Library, 2006.

[9] Youn, W.S.; Un, C.K.: Robust adaptive beamforming based on the eigenstructure method. *IEEE Trans. Signal. Process.*, **42** (6) (1994), 1543–1547.

[10] Bell, K.L.; Ephraim, Y.; Van Trees, H.L.: A bayesian approach to robust adaptive beamforming. *IEEE Trans. Signal. Process.*, **48** (2) (2000), 386–398.

[11] Er, M.H.; Ng, B.: A new approach to robust beamforming in the presence of steering vector errors. *IEEE Trans. Signal. Process.*, **42** (7) (1994), 1826–1829.

[12] Vorobyov, S.A.; Gershman, A.B.; Luo, Z.-Q.: Robust adaptive beamforming using worst-case performance optimization: a solution to the signal mismatch problem. *IEEE Trans. Signal. Process.*, **51** (2) (2003), 313–324.

[13] Li, J.; Stoica, P.; Wang, Z.: On robust capon beamforming and diagonal loading. *IEEE Trans. Signal. Process.*, **51** (7) (2003), 1702–1715.

[14] Yang, F.; Liao, G.; Xu, J.; Zhu, S.; Cao, Z.: Robust adaptive beamforming against large steering vector mismatch using multiple uncertainty sets. *Signal. Process.*, **152** (2018), 320–330.

[15] Li, Y.; Ma, H.; Yu, D.; Cheng, L.: Iterative robust capon beamforming. *Signal Process*, **118** (118) (2016), 211–220.

[16] Li, Y.; Ma, H.; Cheng, L.: Iterative robust adaptive beamforming. *EURASIP. J. Adv. Signal. Process.*, **2017** (1) (2017), 58.

[17] Gu, Y.; Leshem, A.: Robust adaptive beamforming based on interference covariance matrix reconstruction and steering vector estimation. *IEEE Trans. Signal. Process.*, **60** (7) (2012), 3881–3885.

[18] Igambi, D.; Yang, X.; Jalal, B.: Robust adaptive beamforming based on desired signal power reduction and output power of spatial matched filter. *IEEE Access.*, **6** (2018), 50217–50228.

[19] Lu, Z.; Li, Y.; Gao, M.; Zhang, Y.: Interference covariance matrix reconstruction via steering vectors estimation for robust adaptive beamforming. *Electron. Lett.*, **49** (22) (2013), 1373–1374.

[20] Liu, J.; Wei, X.; Guan, G.; Zhang, Q.; Wan, Q.: Adaptive beamforming algorithms with robustness against steering vector mismatch of signals. *IET Radar Sonar & Navigation*, **11** (12) (2017), 1831–1838.

[21] Zhang, Z.; Wei, L.; Wen, L.; Wang, A.; Shi, H.: Interference-plus-noise covariance matrix reconstruction via spatial power spectrum sampling for robust adaptive beamforming. *IEEE Signal Process. Lett.*, **23** (1) (2015), 121–125.

[22] Ganz, M.W.; Moses, R.L.; Wilson, S.L.: Convergence of the smi and the diagonally loaded smi algorithms with weak interference. *IEEE Trans. Antennas Propag.*, **38** (3) (1990), 394–399.

[23] Van Trees, H.L.: Optimum Array Processing Part IV of Detection, Estimation, and Modulation Theory. John Wiley & Sons, Inc., New York, 2002.

[24] Elnashar, A.; Elnoubi, S.M., El-Mikati, H.A.: Further study on robust adaptive beamforming with optimum diagonal loading. *IEEE Trans. Antennas Propag.*, **54** (12) (2006), 3647–3658.

[25] Zhang, L.; Liu, W.: Robust beamforming for coherent signals based on the spatial-smoothing technique. *Signal Process.*, **92** (11) (2012), 2747–2758.

[26] Chang, L.; Yeh, C.-C.: Performance of dmi and eigenspace-based beamformers. *IEEE Trans. Antennas Propag.*, **40** (11) (1992), 1336–1347.

[27] Nai, S.E.; Ser, W.; Yu, Z.L.; Chen, H.: Iterative robust minimum variance beamforming. *IEEE Trans. Signal. Process.*, **59** (4) (2011), 1601–1611.

[28] Zarifi, K.; Shahbazpanahi, S.; Gershman, A.B.; Luo, Z.-Q.: Robust blind multiuser detection based on the worst-case performance optimization of the mmse receiver. *IEEE Trans. Signal. Process.*, **53** (1) (2005), 295–305.

[29] Ali, A.H.; Ye, Q.; Zhuang, J.; Tan, Q.: Low-complexity variable loading for robust adaptive beamforming. *Electron. Lett.*, **52** (5) (2016), 338–340.

[30] Li, Y.; Hong, M.; Wenjun, C.; De, Y.: Improvement of interference covariance matrix reconstruction-based robust adaptive

beamforming, in *Management Information and Optoelectronic Engineering, 2016*. World Scientific, 2016, 3–10.

[31] Wang, W.; Wu, R.; Liang, J.: A novel diagonal loading method for robust adaptive beamforming. *Prog. Electromagnetics Res. C*, **18** (2011), 245–255.

Linxian Liu received the bachelor degree from Hunan Normal University in 2008 and received her master degree from South-Central University for Nationalities in 2011, respectively. She is currently a lecturer of Wuhan College of Foreign Languages and Foreign Affairs. Her main research interests are signal processing and technology English writing.

Yang Li received the B.S. degree in optical information science and technology and the M.S. degree in radio physics from Wuhan University of Technology, Wuhan, China, in 2006 and 2010, respectively, and received the Ph.D. degree in electromagnetic field and microwave technology from Huazhong University of Science and Technology, Wuhan, China, in 2016. He was with the FiberHome Technologies Group, Wuhan, in 2011, and CSIC No.722 Research and Development Institute, Wuhan, in 2016. He is currently a lecturer of School of Electrical and Information Engineering, Wuhan Institute of Technology, Wuhan, China. His research interests include array signal processing, radar signal processing, and radio wave propagation.